Effect of concentration and flow rate of electrolyte on electrochemical regeneration of activated carbon at pilot-plant scale

Borja Ferrández-Gómez [a], Beatriz Martínez-Sánchez [b,d], Diego Cazorla-Amorós [b,c], Emilia Morallón [b,d,*]

[a] Department of Biochemistry and Molecular Biology and Soil Science and Agricultural Chemistry, University of Alicante, 03690 Alicante, Spain
[b] Materials Institute of Alicante, University of Alicante, 03690 Alicante, Spain
[c] Department of Inorganic Chemistry, University of Alicante, 03690 Alicante, Spain
[d] Department of Physical Chemistry, University of Alicante, 03690 Alicante, Spain

ARTICLE INFO

ABSTRACT

Few research has investigated the problem of regeneration of activated carbon once it has been saturated by organic and inorganic contaminants. Among the regeneration methods, electrochemical technology is one of the most advanced, demonstrating its effectiveness in pilot-plant scale experiments using samples obtained from drinking water treatment plants. In the present study, the optimization of a parallel plate electrochemical reactor with a capacity of 15 kg of activated carbon, has been achieved regarding the electrolyte concentration and flow rate. A regeneration efficiency of approximately 90% was achieved with a 0.25 M H_2SO_4 concentration, while lower concentrations resulted in a voltage exceeding the acceptable limits for this type of installation. In addition, higher flow rates imply a higher recovery of the porous texture of the regenerated activated carbon. This is, to the best of our knowledge, the first report where these two experimental variables are optimized in a pilot-scale process with real saturated activated carbon samples with different types of pollutants adsorbed in the activated carbon.

1. Introduction

The development of the World population has led to a growth in industrialization and urbanization which has produced increased levels of pollution in water and air. The contamination in these environments is leading to more health problems, deteriorating levels of air and water quality and habitat modification, being one of the most important factors in climate change [1].

For these reasons, governments are enforcing regulations to set limits on the number of pollutants that can be released and require industries to implement best practices to reduce them. Moreover, some policies to reducing waste and promoting conservation practices to protect the environment are being implemented. Among the most relevant measures, we find the increase of waste management through recycling and circular economy strategies [2] and the development of treatment technologies to diminish pollution levels in air and water such as filtration, oxidation, exchange membranes and the adoption of more energy efficient systems to bring down the footprint [3].

One of the most widely implemented technologies for pollutant removal is the adsorption in activated carbon (AC) [4,5]. In fact, the global consumption market of AC was valued at $3.2 billion in 2020 and was estimated to be around $5.8 billion by 2030 [6]. However, AC has three limitations as an adsorbent of pollutants such as its economic cost when used in industries at large-scale, its disposal as waste and its production processes, since they also produce emissions of greenhouse gases, contributing to environmental degradation [7,8].

Despite these limitations, AC remains a widely used and effective tool for decreasing pollution and different methods to recover its adsorptive properties have been investigated for their recycling, since this approach would reduce waste generation and the environmental impact associated with waste disposal or incineration. There are different methods for regeneration of AC: thermal, chemical, microbiological and vacuum technologies [9]. In addition, advanced methods have been investigated including electrochemical and photo-Fenton, electro-peroxymonosulfate, electro-peroxone, ozonation, hydrothermal hydrogenation, ultraviolet and microwave-assisted regeneration process

[10–22]. However, even though these novel methods offer significant improvements, it is important to carefully consider their limitations (e. g., cost, equipment, efficiency and durability). So, further research is needed to evaluate its effectiveness and feasibility.

Nowadays, one regeneration method that is gaining more interest is electrochemical regeneration, which can be a promising alternative to the thermal treatment due to its high efficiency, selectivity, environmentally friendly, and its scalability into large scale reactors [8,23–26]. To optimize efficiency of electrochemical regeneration, there are several parameters to consider such as regeneration time (e.g., 1–8 h), applied current (e.g., 0.01–2.5 A) and electrode composition (e.g., Pt, stainless steel, carbon-based material, boron-doped diamond, and mixed metal oxides). It should be noted that these factors have been previously optimized both at laboratory and pilot scale with AC samples that were spent under real conditions and in laboratory conditions [10,13,25,27–31].

However, it has been demonstrated that the most important factor to obtain the highest recovery of the AC properties is the electrolyte due to its capability to fix the pH as well as the ionic conductivity. In previous studies at laboratory scale, NaCl, NaBr, KCl, NaOH, NaHCO$_3$, H$_2$SO$_4$, Na$_2$SO$_4$, K$_2$SO$_4$, H$_3$PO$_4$, CH$_3$COONa and water have been used with different efficiencies of regeneration [13,26,32–35].

The third variable related with the electrolyte is the flow rate, a parameter that has not yet been analyzed in pilot-scale electrochemical reactors with AC samples saturated in real conditions such as a drinking water treatment plant (DWTP). It is worth noting that the contact time between the AC and the electrolyte, can affect the efficiency of the removal of contaminants from the AC surface. As far as we know, only one work studied this effect, concluding that fluidization favors desorption of the compounds from the AC [36]; nevertheless, there are no studies conducted at the pilot plant scale or higher, showing the impact of flow rate and electrolyte concentration on regenerating AC in an electrochemical reactor.

Thus, the electrochemical regeneration of AC is a topic of interest in recent years that, despite numerous studies performed, still needs for further investigation to optimize the overall process. The purpose of this work is to study the effect of concentration and flow rate of H$_2$SO$_4$ electrolyte solution in electrochemical regeneration of AC spent in a DWTP in real conditions using an electrochemical reactor at pilot-plant scale with a capacity of 15 kg of AC.

2. Materials and methods

2.1. Materials

The granular AC used in this work was Filtrasorb®TL820 (10x20 mesh, agglomerated, Chemviron Carbon, Belgium) which had been thermally regenerated two times with two *make-up* treatments with 10% Norit1020® (10x20 mesh, agglomerated, Cabot Norit Activated Carbon, The Netherlands). The AC was spent in La Presa municipal DWTP located in Valencia (Spain) for 3 years for the retention of organic compounds as geosmin and 2-methylisoborneol, in unknown concentration, improving the organoleptic properties of water; moreover, inorganic compounds are also adsorbed. Sulfuric acid (H$_2$SO$_4$, VWR International, USA) solution prepared with tap water was used as electrolyte. The electrodes used as anode and cathode have been commercial Ti mesh fully platinized and 304-stainless steel mesh, respectively.

2.2. Electrochemical regeneration of activated carbon

The electrochemical regeneration of ACs was done using the electrochemical reactor prototype designed and built with parallel plate electrode configuration at pilot-plant-scale (Fig. 1). This electrochemical reactor has been previously described by Ferrández-Gómez et al. [25]. Briefly, for each experiment, 15 kg of spent AC were placed into the cathodic compartment using H$_2$SO$_4$ as electrolyte, 75 L in each tank. In all cases the current density used was 0.025 A/cm^2 during 4 h, supplied by a power source (GE050250DVR, Grelco, Spain) operating in galvanostatic mode and the reached voltage was measured at the beginning and the end of the experiments. In this reactor, it is possible to recover almost 100 % of the regenerated activated carbon, being this an advantage compared to thermal regeneration.

To study the effect of electrolyte concentration, the electrochemical regeneration tests were done maintaining the flow rate of electrolyte at 750 L/h with different H$_2$SO$_4$ concentration: 0.5 (PPR-1), 0.1 (PPR-2) and 0.25 M (PPR-3). All experiments carried out to study the effect of electrolyte concentration were done in triplicate.

The effect of flow rate of electrolyte has been studied using 0.5 M of H$_2$SO$_4$ and three different flow rates: 300 (PPR-5), 500 (PPR-1) and 750 L/h (PPR-4). The three experiments performed to study the effect of flow rate were done in triplicate.

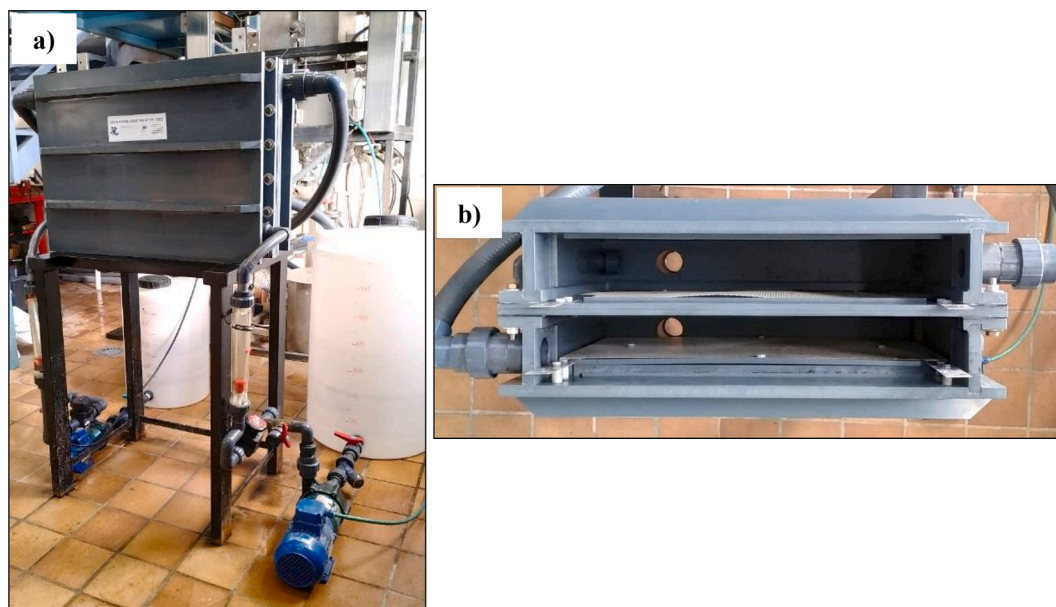Different samples have been taken out at different points of the AC

Fig. 1. A) photograph of parallel plate electrodes prototype at pilot-plant-scale for the electrochemical regeneration of ac and b) top view of electrochemical reactor.

bed and mixed to obtain homogenized samples of regenerated AC. Each sample was washed with abundant distilled water until neutral pH and dried at 70 °C for overnight. In addition, to test the effect of the contact of the AC with the electrolyte in absence of current, 6 g of spent AC was put in contact and in continuous agitation for 1 h with 200 mL of electrolytic aqueous 0.5 M H_2SO_4 solution.

2.3. Characterization of activated carbon

The porous texture of pristine, spent and regenerated AC samples was determined by N_2 adsorption–desorption isotherm at −196 °C and CO_2 adsorption isotherm at 0 °C using an automatic adsorption system (Autosorb-6B, Quantachrome Corporation, USA). The samples were outgassed at 150 °C under vacuum for 8 h. Total volume of micropores ($V_{DR}(N_2)$) and volume of narrow micropores ($V_{DR}(CO_2)$) were calculated applying the Dubinin-Radushkevich (DR) equation [37], the volume of mesopores (V_{meso}) was calculated by subtraction of the adsorbed volume at relative pressures of 0.9 and 0.2 [38] and the apparent specific surface area was determined by the Brunauer-Emmet-Teller (BET) equation [39]. The pore size distribution (PSD) was calculated by applying the bidimensional non-local density functional theory method (2D-NLDFT) to the N_2 adsorption isotherms using SAIEUS software (version 2.0, Micromeritics Instrument Corp. 2000–2015) [40].

The surface chemistry of ACs was analyzed by temperature-programmed desorption (TPD) experiments. These were performed in a DSC-TGA equipment (Simultaneous TGA/DSC SDT Q600, TA Instruments, USA) coupled to a mass spectrometer (HiCube 80 Eco, Pfeiffer Vacuum, Germany) which was used to follow the *m/z* lines related to the decomposition of surface functional groups from the AC. The thermobalance was purged for 1 h under a He flow rate of 100 mL/min and then heated up to 950 °C with a heating rate of 20 °C/min.

In addition, the pH at the point of zero charge (pH_{PZC}) was determined using the procedure previously described by Such-Basáñez et al. [41].

The surface morphology of ACs was studied by scanning electron microscope (SEM) (S-3000N, Hitachi, Japan), which was coupled to a Rontec X-ray detector for energy dispersive X-ray (EDX) analysis.

The electrochemical characterization of ACs was performed by cyclic voltammetry (CV) in a three-electrode cell at 25 °C (controlled by an outer water-jacket) in 0.5 M H_2SO_4 electrolyte N_2-saturated solution in a potential range from 0.2 to 0.8 V at 10 mV/s. An Autolab PGSTAT 302 (Metrohm, Netherlands) potentiostat was used. The electrochemical setup was a standard three-electrode cell, where a reversible hydrogen electrode (RHE) immersed in the working solution through a Luggin capillary was employed as the reference electrode. A graphite bar (supplied by Mersen Ibérica) was used as a counter electrode. The working electrode (WE) consists of a glassy carbon disk (5 mm of diameter) as support, previously polished with alumina slurries and rinsed with ultrapure water. Afterwards, the WE was modified by dropping 1 mg/mL dispersion of each sample in an aqueous solution (20 vol% isopropanol, 79 vol% water and 1 vol% Nafion®). The dispersion was previously homogenized via ultrasonication for at least 30 min. The amount of sample loading on the disk electrode was set to 1.02 mg/cm².

The electrochemical impedance spectroscopy (EIS) analysis was performed at 0.4 V (vs RHE). Data were collected in the frequency range of 10 mHz to 100 kHz with an amplitude for the potential signal of 10 mV in a 0.5 M H_2SO_4 solution. EIS experiments were carried out using the same three-electrode electrochemical cell.

The gravimetric capacitance (C_g) has been calculated from the electrical charge measured in the integration of voltametric profile and divided by the potential range. The specific capacitance was calculated dividing C_g by the S_{BET}.

2.4. Evaluation of the efficiency of electrochemical regeneration

The percentage of regeneration efficiency was determined by calculating the porosity recovery (%RP) as the ratio of regenerated to pristine AC surface area (S_{BET}) according to the Eq. (1). In this work, it was considered that the regeneration of the activated carbon was obtained when the %RP was, as minimum, a value of 85.

$$\%RP = \frac{S_{BET, \, regenerated \, AC}}{S_{BET, \, pristine \, AC}} \cdot 100 \tag{1}$$

3. Results and discussion

3.1. Effect of electrolyte concentration

To elucidate the behavior of H_2SO_4 concentration, PPR-1 (0.5 M) can be considered the reference experiment. In PPR-2 a reduction in concentration of 80% was applied and, for PPR-3 a 50% of reduction was used. It is important to highlight that all the electrochemical regeneration experiments lasted for four hours except for PPR-2, which had to be stopped after the first hour of treatment due to the high voltage reached (27.6 V), since it exceeded the maximum value of 25.0 V allowed by the current Spanish legislation in DWTP facilities.

Fig. 2 presents the N_2 adsorption–desorption isotherms of the pristine, spent, after acid washing (non-electrochemical regeneration) and electrochemically regenerated ACs using different H_2SO_4 concentrations. PSD determined by application of 2D-NLDFT method are also plotted in Fig. 2. As it can be seen, all the isotherms were of type I [42] corresponding to microporous ACs; the small slope for the relative pressure above 0.2 and the small hysteresis cycle shows that the mesopores contribution is low.

Table 1 summarizes the main textural properties, such as the S_{BET}, $V_{DR}(N_2)$, $V_{DR}(CO_2)$, V_{meso}, pH_{PZC}, as well as the %RP, the reached voltage at the end of the experiments (AE), and the amount and types of oxygen-containing surface groups in the carbon materials (CO_2-type and CO-type groups and total oxygen content, O determined as CO + 2CO₂.

It can be observed that the washing with the electrolyte (washed sample) cannot recover the porosity of the pristine activated carbon. Then, this regeneration procedure is not adequate for the regeneration of this spent AC.

Regarding the effect of electrolyte concentration in electrochemically regenerated samples, (PPR-1, PPR-2 and PPR-3 experiments at 500 L/h), in all the cases, a recovery of the porosity was observed for the AC after the electrochemical regeneration compared to the spent AC. It must be noted that, in many cases, the electrochemical treatment was able to recover the PSD of the pristine AC (Fig. 2). The values of %RP were, in the first two hours of experiment, 88, 89 and 98 for PPR-1, PPR-2 and PPR-3, respectively. In all cases, the %RP was above 87 at the end of the electrochemical process. Regarding regeneration time, for electrolyte concentration study, the behavior was similar to that previously published by different authors [25,26,28,35], who found that for this type of electrochemical process there was a rapid increase in regeneration efficiency in the first three hours until reaching a constant value.

The surface chemistry of the pristine, spent, washed and regenerated ACs was characterized by TPD experiments and by measurement of pH_{PZC} (Table 1) in order to check the oxidation degree of the regenerated materials after electrochemical treatment.

Pristine AC had a low amount of surface oxygen groups and an alkaline pH_{PZC} value, while the spent AC had a much higher CO and CO_2 evolution and a lower pH_{PZC}. This reveals that the AC was oxidized during the use in the DWTP and by the two thermal regeneration treatments carried out, what is in agreement with what has been previously concluded for a sample from another DWTP [25]. In addition, Fig. 3 shows that some of the gas desorbed could be due to the decomposition of inorganic compounds like metal carbonates (this is clearly observed in the peak at 650–700 °C in the CO_2 profile in Fig. 3 for spent AC). This is reasonable considering that the analysis of the spent AC by EDX and SEM (Table S1 and Fig. S3) shows the presence of calcium in a significant amount (4.95 wt%). The TPD profile for the spent AC after
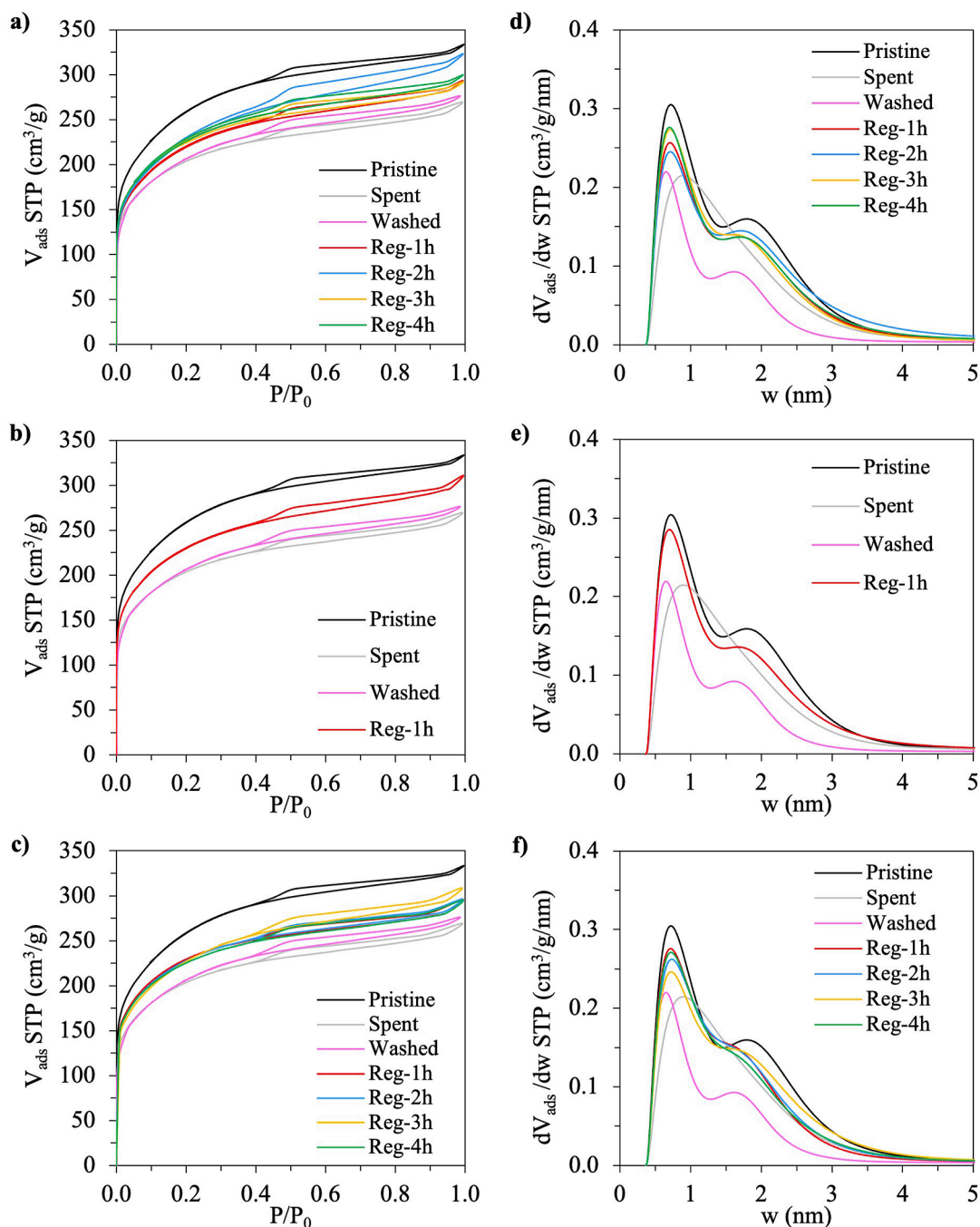
Fig. 2. A), b) and c) n$_2$ adsorption–desorption isotherms at −196 °C and d), e) and f) pore size distribution for samples obtained from the experiments carried out in electrochemical regeneration of AC for the optimization of electrolyte concentration: a) and d) PPR-1 (0.5 M H$_2$SO$_4$), b) and e) PPR-2 (0.1 M H$_2$SO$_4$) and c) and f) PPR-3 (0.25 M H$_2$SO$_4$). The data for pristine, spent and acid washed AC are also included for comparison purposes.

washing and after the electrochemical treatments with the acid electrolyte, showed the disappearance of the CO$_2$ peak associated to metal carbonates decomposition (Fig. 3). In any case, the TPD and the pHpzc of the spent AC after washing (Table 1 and Fig. 3) confirms that oxidation of the AC occurred during its use in the DWTP.

The surface chemistry of the electrochemically regenerated ACs using different H$_2$SO$_4$ concentrations, can be compared with the pristine and spent AC after washing because all of them are free of the inorganic species that produce additional features in the TPD. It is important to highlight that the regeneration treatments at these conditions did not produce an important change in CO and CO$_2$ desorption with respect to the washed AC (Fig. 3 and Table 1). It must also be noted that the pH$_{PZC}$

for the regenerated samples was higher than for the acid washed sample, showing that the electrochemical treatment at these conditions was not producing an additional important oxidation of the spent AC. However, among the four regenerated samples obtained for each experiment there were no significant differences in the values of pH$_{PZC}$ or TPD. A similar behavior was reported by other researchers where neither the pH$_{PZC}$ nor the amount of oxygen surface groups of the AC cloth were significantly modified after prolonged negative polarization [43]. Finally, it should also be noted that the lower the electrolyte concentration, the higher the reached voltage due to the increase in electrode resistance (Table 1). This produced an increase in the pH$_{PZC}$ and in the amount of CO type groups (that is, some additional surface oxidation occurs), as well as a

Table 1

Physicochemical characterization of textural properties by N_2 and CO_2 adsorption–desorption isotherms, TPD, pH_{PZC} and AE of pristine, spent and electrochemically regenerated ACs for study of the effect of electrolyte concentration and the flow rate.

Sample	S_{BET} m²/g	V_{DR},N_2 cm³/g	V_{DR},CO_2 cm³/g	V_{meso} cm³/g	%RP	CO µmol/g	CO_2 µmol/g	O µmol/g	pH_{PZC}	AE V
Pristine	950	0.33	0.17	0.09		645	265	1175	11.8	
Spent	750	0.28	0.14	0.08		1875	915	3705	7.8	
Washed	770	0.28	0.15	0.09	80	2210	770	3750	2.0	
PPR-1 (0.5 M H_2SO_4 and 500 L/h)										
Reg-1h	815	0.27	0.19	0.09	86	1875	850	3580	2.6	8.2
Reg-2 h	835	0.29	0.20	0.09	88	2075	870	3815	2.5	7.4
Reg-3 h	825	0.31	0.20	0.09	87	1905	835	3570	2.5	7.1
Reg-4 h	830	0.30	0.20	0.09	87	2200	905	4015	2.6	7.0
PPR-2 (0.1 M H_2SO_4 and 500 L/h)										
Reg-1h	840	0.33	0.20	0.10	88	2505	850	4200	4.9	27.6
PPR-3 (0.25 M H_2SO_4 and 500 L/h)										
Reg-1h	845	0.34	0.19	0.07	89	2090	705	3500	4.1	10.4
Reg-2 h	840	0.33	0.21	0.08	88	2470	760	3985	3.7	10.2
Reg-3 h	835	0.33	0.19	0.10	88	2295	725	3745	3.2	9.9
Reg-4 h	825	0.33	0.19	0.08	87	2620	1060	4740	3.0	9.7
PPR-4 (0.5 M H_2SO_4 and 750 L/h)										
Reg-1h	880	0.32	0.21	0.09	93	2710	940	4590	2.8	7.2
Reg-2 h	815	0.30	0.19	0.09	86	2985	980	4945	2.8	6.5
Reg-3 h	885	0.33	0.20	0.10	93	2580	905	4385	2.7	6.5
Reg-4 h	855	0.32	0.21	0.09	90	2640	930	4505	2.6	6.4
PPR-5 (0.5 M H_2SO_4 and 300 L/h)										
Reg-1h	815	0.32	0.21	0.08	86	2375	925	4230	3.0	6.5
Reg-2 h	795	0.31	0.21	0.08	84	2435	885	4210	2.6	6.2
Reg-3 h	805	0.32	0.18	0.07	85	2380	840	4065	2.6	5.8
Reg-4 h	810	0.31	0.19	0.08	85	2235	670	3580	2.4	5.7

small increase in the porosity for the regenerated samples (as observed in the increase in the V_{DR},N_2).

Considering the %RP, in this study, it seems that the most adequate electrolyte concentration was 0.25 M due to the better recovery of porous texture (from 750 m²/g to 845 m²/g after 1 h of electrochemical treatment) compared to 0.5 M (from 750 m²/g to 835 m²/g in 2 h of electrochemical treatment). Besides, 0.25 M could be considered as a better option taking into account the economic and environmental cost of the electrochemical regeneration of AC under these experimental conditions. However, the higher voltage reached for 0.25 M (10.4–9.7 V) compared to 0.5 M (8.2–7.0 V), will result in higher energy consumption to carry out the electrochemical regeneration process with its economic cost associated, and this will have to be taken into account in the studies of life cycle assessment and life cycle cost. Finally, even though the 0.1 M concentration had similar %RP values to the 0.25 and 0.5 M, this concentration was discarded due to the high voltage (27.6 V) reached during the electrochemical regeneration.

Gazigil et al. [32] explains that this fact may be due to the fact that the driving force of the electrolytic reaction decreases when the applied voltage is gradually reduced as the electrolyte concentration increases. Moreover, and according with Ye et al. [44], when the electrolyte concentration is increased, the ions adsorbed on the electrode from the electrolyte can block active sites, inhibiting the formation of ·OH radicals and consequently, decreasing the %RP.

A similar electrolyte concentration effect was studied by Khataee et al. [45] for Na_2SO_4, concluding there was a need for higher voltages to overcome the decrease in the electrical conductivity, being a non-viable option with low concentrations.

However, this behavior is contrary to that concluded by different authors who described that the higher the concentration the higher the regeneration achieved [32,33,35,46]. This difference could be due to the reactor configuration and AC amount to regenerate, as these are fixed beds and our work is done using a moving bed where the recirculation of the electrolyte increases the mass transfer. Another explanation could be the proposed by McQuillan et al. [26] who suggest that once a certain current density is exceeded using a particular electrolyte concentration, regeneration efficiencies tend to stabilize, or sometimes decrease, due to the increased number of by-product reactions that occur.

3.2. Optimization of flow rate of electrolyte

An important parameter that may affect to the %RP of ACs is the electrolyte flow rate. To study this effect, three experiments were carried out using 750 (PPR-4), 500 (PPR-1) and 300 L/h (PPR-5), which corresponds to residence times of 168, 252 and 420 s, respectively.

As can be seen in Table 1, the %RP was 86, 88 and 93 for PPR-5, PPR-1 and PPR-4, as the flow rate increases, respectively. Regarding regeneration time, the trend is similar to that obtained for the effect of electrolyte concentration, where a maximum regeneration is reached in the first hour of treatment and then maintained with slight variations that are not significant until the end of the test.

Fig. S1 contains the N_2 adsorption–desorption isotherms and the PSD for the different materials obtained for this study. The results show that the isotherms for the electrochemically regenerated ACs have a similar shape but an increase in the adsorption capacity compared to the spent sample in the three tests performed. Regarding PSD, as occurred in the study of the effect of electrolyte concentration, this treatment produced an almost complete recovery of porosity compared to the original sample. The differences between the regenerated samples were observed in the microporous region (Table 1 and Fig. S1) and the electrolyte flow rate had no effect on the reached voltage (Table 1).

Interestingly, the regeneration treatments at these conditions produced an important change in CO and CO_2 desorption with respect to the washed AC in experiments done with higher flow rates, where an increase in surface oxygen groups was observed for samples obtained from PPR-4 and PPR-5 experiments (Fig. S2 and Table 1).

Furthermore, as can be seen in Fig. 4, after the 3rd h of treatment, the higher the electrolyte flow rate, the higher the recovery of the porosity.

It is well-known that the electrolyte flow rate is related to the mass transfer rate, which may affect the oxidation, adsorption and desorption processes occurring in the AC [18,36,47,48]. The results showed that an increase in flow rate favors the removal of desorbed compounds resulting in an increase in the porous texture and the %RP (Table 1). This behavior is in agreement with McQuillan et al. [49] where a higher flow rate of the regenerant solution in a carbon-packed column resulted in a higher desorption rate. In addition, Zhou and Lei [36] concluded that, with low electrolyte flow, organic compounds retained in AC could
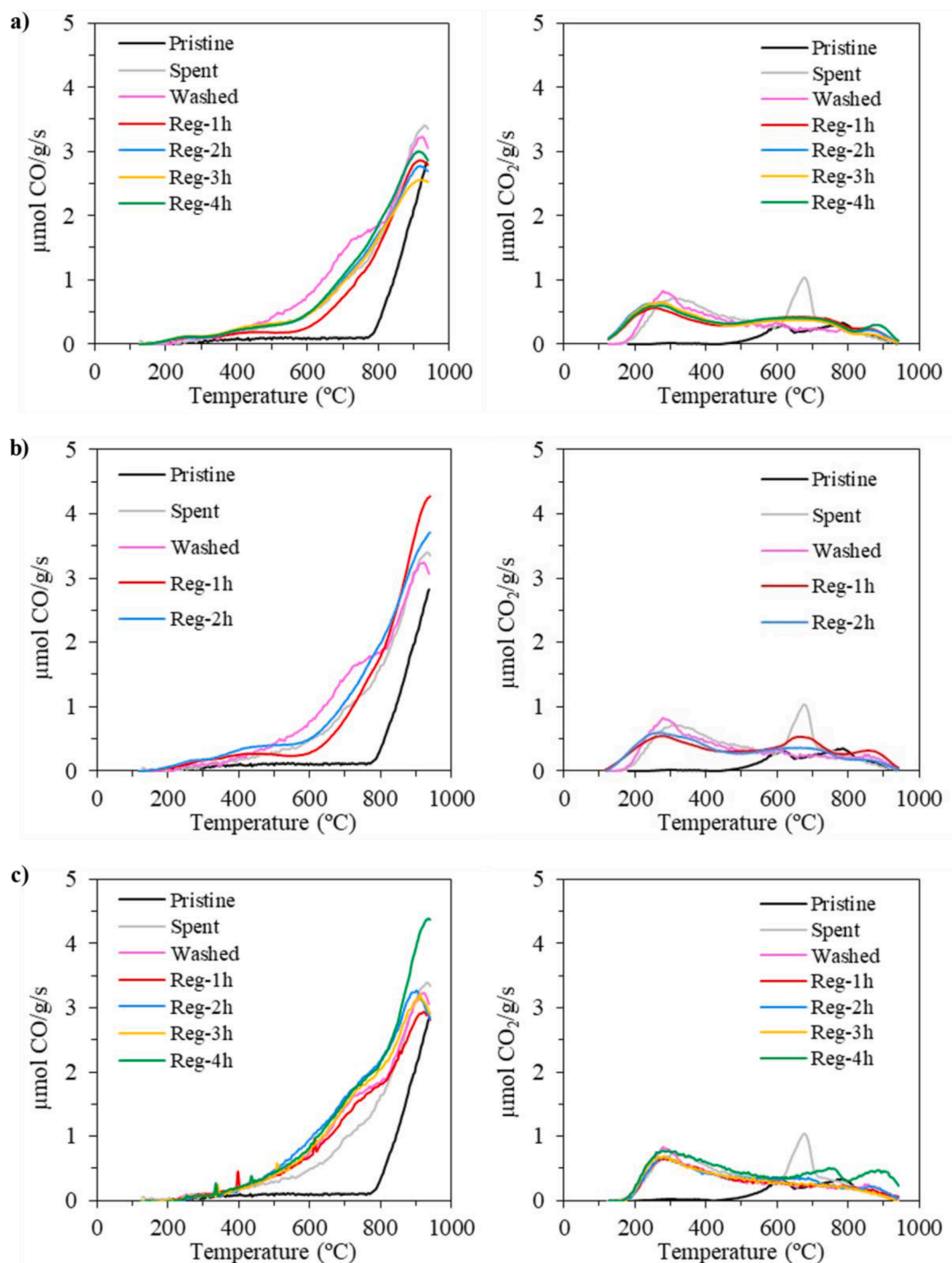
Fig. 3. CO and CO_2 TPD evolution profiles of the ACs regenerated electrochemically from samples obtained for the optimization of electrolyte concentration: a) PPR-1 (0.5 M), b) PPR-2 (0.1 M) and c) PPR-3 (0.25 M). The data for pristine, spent and acid washed AC are also included for comparison purposes.

not be easily attacked by hydroxyl radicals or other generated oxidizing agents, because they could not be efficiently distributed through the electrolyte. However, with the increase in flow rate, the mass transfer is improved, and the AC desorption pathway and oxidizing species diffusion are enhanced. Another explanation that reinforces the results obtained is that a higher flow rate favors the homogenization of pH, directly influencing the processes of electron transfer and mass transport [47], which also can affect the current and energy efficiencies [50].

3.3. Electrochemical characterization of activated carbon

The electrochemical behavior of pristine, spent and regenerated ACs (PPR-3 and PPR-4, after 1 h of treatment) was characterized in a three-electrode cell in acid media. Firstly, the open circuit potential (OCP) of these carbon materials was measured, as seen in Table 2. All OCPs for spent, PPR-3 (Reg-1h) and PPR-4 (Reg-1h) ACs are slightly higher to that of pristine AC, what is in agreement with the higher amount of surface oxygen groups observed in the TPD experiments (Table 1). Fig. 5 shows the CVs obtained, where a rectangular shape can be appreciated for pristine AC as a consequence of the charge and discharge of the electric
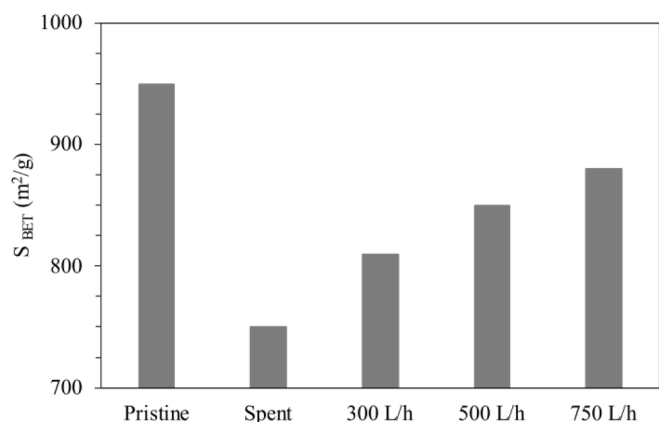
Fig. 4. Effect of flow rate of electrolyte for electrochemical regeneration of AC.

Table 2
OCP, gravimetric (C_g) and surface capacitance (C_g/S_{BET}), equivalent series resistance (ESR) and ESR plus the equivalent distributed resistance (ESR + EDR) of pristine, spent, PPR-3 (Reg-1h) and PPR-4 (Reg-1h) ACs measured in 0.5 M H_2SO_4.

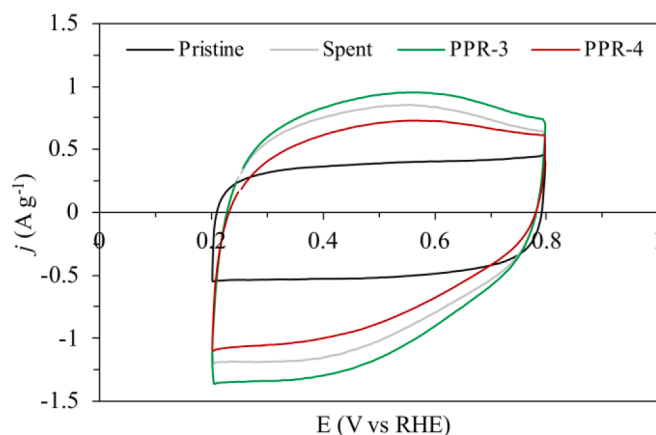| Sample	OCP V (vs RHE)	C_g [10 mV/s] F/g	C_g/S_{BET} [10 mV/s] mF/m^2	ESR Ω	ESR + EDR Ω
Pristine	0.66	42	44	35.2	58.6
Spent	0.71	77	102	78.6	110.2
PPR-3 (Reg-1h)	0.69	86	102	31.8	63.1
PPR-4 (Reg-1h)	0.71	66	74	28.9	70.8

Fig. 5. Cyclic voltammograms for pristine, spent and regenerated ACs (PPR-3 and PPR-4, after 1 h of treatment).

double-layer. A broad redox contribution appears at around 0.5–0.6 V in spent, PPR-3 (Reg-1h) and PPR-4 (Reg-1h) ACs, which could correspond to electroactive surface oxygen-related species [51], thus confirming the oxidation of AC during its use in the DWTP. The less rectangular shape of the CV may also be related to the lower electrical conductivity of the spent AC in presence of impurities. However, it can be observed that the regenerated PPR-3 (Reg-1h) sample shows an increase in voltametric profile compared to spent AC. However, in the case of PPR-4 (Reg-1h) the voltametric profile decreases compared to the spent AC.

Table 2 also shows differences in the calculated gravimetric capacitance (C_g) and specific capacitance (C_g/S_{BET}) for all the samples due to the different surface chemistry and surface area. In the spent and

electrochemically regenerated samples, the capacitance increases in comparison to the pristine AC. The increase in capacitance for spent, PPR-3 (Reg-1h) can be ascribed to two factors: (i) the increase of the double-layer capacitance due to high electrochemical accessible area, possibly related to an improvement of carbon wettability, and (ii) the pseudocapacitive contribution of the redox processes due to electro-active surface species. It is well-known that CO-evolving groups are beneficial for increasing the wettability of carbon materials [51]. Interestingly, PPR-4 (Reg-1h) AC presents capacitance values lower than the spent AC, this result can be explained as consequence of the increased oxidation of this sample during electrochemical regeneration as consequence of the higher sulphuric acid concentration (Table 1). This oxidation can block the porosity of the activated carbon decreasing the capacitance.

Fig. 6 shows the Nyquist plot obtained for the ACs, where important differences are observed. At high frequencies of the Nyquist plot (i.e., impedance values closer to the -Z'' axis), the materials behave as a resistance. At this region, the impedance determined by the first inter-cept of the Z' axis (known as the internal resistance or equivalent series resistance, ESR) is due to the ohmic resistance of the electrolyte between the working and the reference electrodes, together with the resistance of the electrode and the contact between the current collector and the electrode [52]. Since the same electrochemical setup, procedure and material weight have been used in all measurements, we propose that the main differences observed in ESR values in Table 2 could be related to the inherent electrical conductivity of the carbon materials studied. Similar ESR values are observed for PPR-3 (Reg-1h) and PPR-4 (Reg-1h) and the pristine AC, whereas spent AC shows the highest resistance probably due to the oxidation of the material in the DWTP and the presence of inorganic compounds and adsorbed species at the surface that increase the electrical resistance of the material. Therefore, it is evidenced that the electrochemical regeneration treatment allows to recover the electrical conductivity of the pristine AC after the first hour of treatment.

At the middle-low frequency domain, a semicircle is not observed in any sample, thus indicating that charge transfer processes do not occur at the electrode under the conditions studied. Instead, the presence of a Warburg region, represented by an approximately 45° line, evidences the ion diffusion limitation process to the porous electrode surface [53], this resistance is also known as the equivalent distributed resistance (EDR). Finally, the lowest frequency region consists of an almost vertical line attributed to the dominant capacitive behavior [54]. As seen in Fig. 6, the onset frequency for obtaining such capacitive behavior is higher in spent AC than in pristine AC, while less vertical line is observed for PPR-3 (Reg-1h) and PPR-4 (Reg-1h) samples at low frequencies. Table 2 also includes the ESR + EDR values, determined from the x-intercept of this line, which could also be interpreted as an indicator of
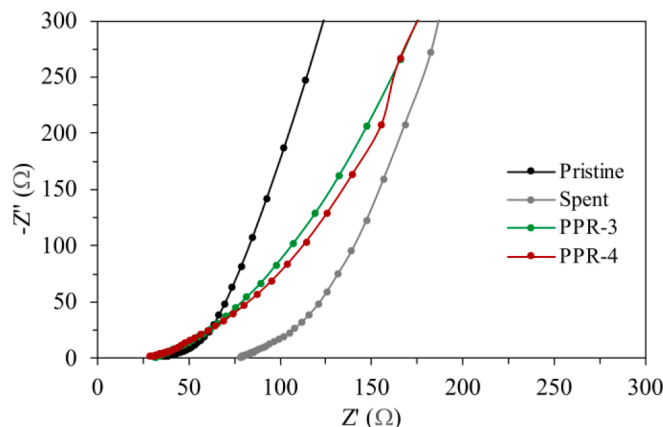

Fig. 6. Nyquist plot obtained for the different ACs studied.

the resistance of the ACs at 0.4 V (vs RHE) in acid media, in agreement with the above discussion. Then, it can be observed that this value is lower in the case of PPR-3 (Reg-1h) which has been electrochemically regenerated using 0.25 M H_2SO_4.

4. Conclusions

The electrochemical regeneration of spent AC used in a DWTP can be achieved using the designed pilot-plant-scale parallel-plane electrode reactor that operates with 15 kg of AC. Under ideal experimental conditions, a recovery of porosity of approximately 93% was obtained for the regenerated activated carbon.

From our findings, it can be concluded that washing with a 0.5 M H_2SO_4 electrolyte is ineffective in recovering the porosity of the AC. Therefore, this chemical regeneration method is not suitable for the spent AC that has undergone two previous thermal regeneration treatments.

The electrochemical characterization of the spent and regenerated samples using cyclic voltammetry and EIS shows that in the DWTP, the pristine activated carbon has been oxidized in the previous water treatment step using chlorine; this disinfection step alters the AC properties. However, the electrochemical regeneration can improve the textural properties and the electrochemical properties improving the conductivity and porosity recovery of the spent activated carbons.

The optimal electrolyte concentration depends on the reached voltage in the electrochemical reactor. In this study, a concentration of 0.1 M H_2SO_4 is not adequate due to the high voltage obtained in the reactor. When analyzing 0.5 M and 0.25 M concentrations, the last value is established as the optimum value. This concentration in the electrochemical regeneration of spent AC it is an alternative that generates fewer by-products and waste, as well as a reduced volume of H_2SO_4. In these conditions, a regeneration efficiency of 89% is achieved within just 1 h of treatment.

Concerning the flow rate of the electrolyte, the higher the flow rate, the higher the recovery of textural properties of the regenerated AC is reached. It should be noted that although a slight oxidation of the material was observed at a flow rate of 750 L/h, the regeneration time is not a significant factor in this oxidation process of the material.

CRediT authorship contribution statement

Borja Ferrández-Gómez: Conceptualization, Methodology, Investigation, Writing – original draft. **Beatriz Martínez-Sánchez:** Investigation, Writing – original draft. **Diego Cazorla-Amorós:** Conceptualization, Methodology, Supervision, Writing – review & editing, Funding acquisition. **Emilia Morallón:** Conceptualization, Methodology, Project administration, Supervision, Writing – review & editing, Funding acquisition.

Declaration of Competing Interest

The authors declare that they have no known competing financial interests or personal relationships that could have appeared to influence the work reported in this paper.

Data availability

Data will be made available on request.

Acknowledgements

Appendix A. Supplementary data

Supplementary data to this article can be found online at https://doi.org/10.1016/j.jelechem.2023.117727.

References

[1] P.D. Noyes, M.K. McElwee, H.D. Miller, B.W. Clark, L.A. Van Tiem, K.C. Walcott, K.N. Erwin, E.D. Levin, The toxicology of climate change: environmental contaminants in a warming world, Environ. Int. 35 (2009) 971–986, https://doi.org/10.1016/j.envint.2009.02.006.

[2] K. Winans, A. Kendall, H. Deng, The history and current applications of the circular economy concept, Renew. Sustain. Energy Rev. 68 (2017) 825–833, https://doi.org/10.1016/j.rser.2016.09.123.

[3] P.R. Rout, T.C. Zhang, P. Bhunia, R.Y. Surampalli, Treatment technologies for emerging contaminants in wastewater treatment plants: A review, Sci. Total Environ. 753 (2021), 141990, https://doi.org/10.1016/j.scitotenv.2020.141990.

[4] C.C. Murray, H. Vatankhah, C.A. McDonough, A. Nickerson, T.T. Hedtke, T.Y. Cath, C.P. Higgins, C.L. Bellona, Removal of per- and polyfluoroalkyl substances using super-fine powder activated carbon and ceramic membrane filtration, J. Hazard. Mater. 366 (2019) 160–168, https://doi.org/10.1016/j.jhazmat.2018.11.050.

[5] J. Rivera-Utrilla, M. Sánchez-Polo, V. Gómez-Serrano, P.M. Álvarez, M.C.M. Alvim-Ferraz, J.M. Dias, Activated carbon modifications to enhance its water treatment applications. An overview, J. Hazard. Mater. 187 (2011) 1–23, https://doi.org/10.1016/j.jhazmat.2011.01.033.

[6] M. Pratik, P. Bhagyashri, P. Yerukola, Activated carbon market by product type (powdered activated carbon, granular activated carbon, others), by application (liquid phase, gaseous phase), by end-use industry (water treatment, food & beverage, pharmaceutical & medical, automotive, air purification, others): Global Opportunity Analysis and Industry Forecast, 2020-2030, 2022.

[7] G. Crini, E. Lichtfouse, L.D. Wilson, N. Morin-Crini, Conventional and non-conventional adsorbents for wastewater treatment, Environ. Chem. Lett. 17 (2019) 195–213, https://doi.org/10.1007/s10311-018-0786-8.

[8] W. Zhou, X. Meng, J. Gao, H. Zhao, G. Zhao, J. Ma, Electrochemical regeneration of carbon-based adsorbents: a review of regeneration mechanisms, reactors, and future prospects, Chem. Eng. J. Adv. 5 (2021) 100083, https://doi.org/10.1016/j.ceja.2020.100083.

[9] F. Salvador, N. Martin-Sanchez, R. Sanchez-Hernandez, M.J. Sanchez-Montero, C. Izquierdo, Regeneration of carbonaceous adsorbents. Part I: Thermal regeneration, Microporous Mesoporous Mater. 202 (2015) 259–276, https://doi.org/10.1016/j.micromeso.2014.02.045.

[10] R. Berenguer, J.P. Marco-Lozar, C. Quijada, D. Cazorla-Amorós, E. Morallón, Effect of electrochemical treatments on the surface chemistry of activated carbon, Carbon 47 (2009) 1018–1027, https://doi.org/10.1016/j.carbon.2008.12.022.

[11] N.A. Bury, K.A. Mumford, G.W. Stevens, The electro-Fenton regeneration of Granular Activated Carbons: degradation of organic contaminants and the relationship to the carbon surface, J. Hazard. Mater. 416 (2021), 125792, https://doi.org/10.1016/j.jhazmat.2021.125792.

[12] H. Ding, Y. Zhu, Y. Wu, J. Zhang, H. Deng, H. Zheng, Z. Liu, C. Zhao, In situ regeneration of phenol-saturated activated carbon fiber by an electro-peroxymonosulfate process, Environ. Sci. Tech. 54 (2020) 10944–10953, https://doi.org/10.1021/acs.est.0c03766.

[13] B. Ferrández-Gómez, R. Ruiz-Rosas, S. Beaumont, D. Cazorla-Amorós, E. Morallón, Electrochemical regeneration of spent activated carbon from drinking water treatment plant at different scale reactors, Chemosphere 264 (2021) 128399, https://doi.org/10.1016/j.chemosphere.2020.128399.

[14] O. Garcia-Rodriguez, A. Villot, H. Olvera-Vargas, C. Gerente, Y. Andres, O. Lefebvre, Impact of the saturation level on the electrochemical regeneration of activated carbon in a single sequential reactor, Carbon 163 (2020) 265–275, https://doi.org/10.1016/j.carbon.2020.02.041.

[15] Z. Liu, B. Ren, H. Ding, H. He, H. Deng, C. Zhao, P. Wang, D.D. Dionysiou, Simultaneous regeneration of cathodic activated carbon fiber and mineralization of desorbed contaminations by electro-peroxydisulfate process: Advantages and limitations, Water Res. 171 (2020) 115456, https://doi.org/10.1016/j.watres.2019.115456.

[16] M. Ren, J. Wang, Z. Wang, S. Sun, J. Qiu, Y. Shi, Z.-J. Wang, Y. Xie, Activated carbon adsorption coupled with ozonation regeneration for efficient removal of chlorobenzene, J. Environ. Chem. Eng. 10 (2) (2022) 107319.

[17] D.H.S. Santos, J.L.S. Duarte, J. Tonholo, L. Meili, C.L.P.S. Zanta, Saturated activated carbon regeneration by UV-light, H_2O_2 and Fenton reaction, Sep. Purif. Technol. 250 (2020) 117112, https://doi.org/10.1016/j.seppur.2020.117112.

[18] H. Sun, Z. Liu, Y. Wang, Y. Li, Electrochemical in situ regeneration of granular activated carbon using a three-dimensional reactor, J. Environ. Sci. 25 (2013) S77–S79, https://doi.org/10.1016/S1001-0742(14)60630-6.

[19] C. Trellu, B.P. Chaplin, C. Coetsier, R. Esmilaire, S. Cerneaux, C. Causserand, M. Cretin, Electro-oxidation of organic pollutants by reactive electrochemical membranes, Chemosphere 208 (2018) 159–175, https://doi.org/10.1016/j.chemosphere.2018.05.026.

[20] X. Wang, Y. Qian, H. Chen, X. Li, A. Zhang, X. Li, C. Chen, Y. He, G. Xue, Achieving multi-cycle regeneration of activated carbon and Cr(VI) removal over a wide pH range by hydrothermal converting quinonimine dye into difunctional pyrrolic-N: Implication for carbon capture in printing and dyeing wastewater treatment, Chem. Eng. J. 459 (2023), 141646, https://doi.org/10.1016/j.cej.2023.141646.

[21] Y. Xiao, J.M. Hill, Mechanistic insights for the electro-Fenton regeneration of carbon materials saturated with methyl orange: dominance of electrodesorption, J. Hazard. Mater. 367 (2019) 59–67, https://doi.org/10.1016/j.jhazmat.2018.12.066.

[22] J. Zhan, Y. Wang, H. Wang, W. Shen, X. Pan, J. Wang, G. Yu, Electro-peroxone regeneration of phenol-saturated activated carbon: The effects of irreversible adsorption and operational parameters, Carbon 109 (2016) 321–330, https://doi.org/10.1016/j.carbon.2016.08.034.

[23] R. Berenguer, J.P. Marco-Lozar, C. Quijada, D. Cazorla-Amorós, E. Morallón, Comparison among chemical, thermal, and electrochemical regeneration of phenol-saturated activated carbon, Energy Fuels 24 (2010) 3366–3372, https://doi.org/10.1021/ef901510c.

[24] G. Ersan, G.A. Cerrón-Calle, M.S. Ersan, S. Garcia-Segura, Opportunities for in situ electro-regeneration of organic contaminant-laden carbonaceous adsorbents, Water Res. 232 (2023), 119718, https://doi.org/10.1016/j.watres.2023.119718.

[25] B. Ferrández-Gómez, D. Cazorla-Amorós, E. Morallón, Feasibility of electrochemical regeneration of activated carbon used in drinking water treatment plant. Reactor configuration design at a pilot scale, Process Saf. Environ. Prot. 148 (2021) 846–857, https://doi.org/10.1016/j.psep.2021.02.007.

[26] R.V. McQuillan, G.W. Stevens, K.A. Mumford, The electrochemical regeneration of granular activated carbons: A review, J. Hazard. Mater. 355 (2018) 34–49, https://doi.org/10.1016/j.jhazmat.2018.04.079.

[27] C.E. Alvarez-Pugliese, J. Acuña-Bedoya, S. Vivas-Galarza, L.A. Prado-Arce, N. Marriaga-Cabrales, Electrolytic regeneration of granular activated carbon saturated with diclofenac using BDD anodes, Diam. Relat. Mater. 93 (2019) 193–199, https://doi.org/10.1016/j.diamond.2019.02.018.

[28] R.M. Narbaitz, A. Karimi-Jashni, Electrochemical regeneration of granular activated carbons loaded with phenol and natural organic matter, Environ. Technol. 30 (2009) 27–36, https://doi.org/10.1080/09593330802422803.

[29] R.M. Narbaitz, A. Karimi-Jashni, Electrochemical reactivation of granular activated carbon: Impact of reactor configuration, Chem. Eng. J. 197 (2012) 414–423, https://doi.org/10.1016/j.cej.2012.05.049.

[30] L. Wang, N. Balasubramanian, Electrochemical regeneration of granular activated carbon saturated with organic compounds, Chem. Eng. J. 155 (2009) 763–768, https://doi.org/10.1016/j.cej.2009.09.020.

[31] C.-H. Weng, M.-C. Hsu, Regeneration of granular activated carbon by an electrochemical process, Sep. Purif. Technol. 64 (2008) 227–236, https://doi.org/10.1016/j.seppur.2008.10.006.

[32] L. Gazigil, E. Er, T. Yonar, Determination of the optimum conditions for electrochemical regeneration of exhausted activated carbon, Diam. Relat. Mater. 133 (2023), 109741, https://doi.org/10.1016/j.diamond.2023.109741.

[33] R.M. Narbaitz, J. Cen, Electrochemical regeneration of granular activated carbon, Water Res. 28 (1994) 1771–1778, https://doi.org/10.1016/0043-1354(94)90250-X.

[34] D.H.S. Santos, J.P.T.S. Santos, J.L.S. Duarte, L.M.T.M. Oliveira, J. Tonholo, L. Meili, C.L.P.S. Zanta, Regeneration of activated carbon adsorbent by anodic and cathodic electrochemical process, Process Saf. Environ. Prot. 159 (2022) 1150–1163, https://doi.org/10.1016/j.psep.2022.01.083.

[35] H. Zhang, Regeneration of exhausted activated carbon by electrochemical method, Chem. Eng. J. 85 (2002) 81–85, https://doi.org/10.1016/S1385-8947(01)00176-0.

[36] M.H. Zhou, L.C. Lei, Electrochemical regeneration of activated carbon loaded with p-nitrophenol in a fluidized electrochemical reactor, Electrochim. Acta 51 (2006) 4489–4496, https://doi.org/10.1016/j.electacta.2005.12.028.

[37] M.M. Dubinin, The potential theory of adsorption of gases and vapors for adsorbents with energetically nonuniform surfaces, Chem. Rev. 60 (1960) 235–241, https://doi.org/10.1021/cr60204a006.

[38] L.J. Lemus-Yegres, M.C. Román-Martínez, I. Such-Basáñez, C. Salinas-Martínez De Lecea, Effects of confinement in hybrid diamine-Rh complex-carbon catalysts used for hydrogenation reactions, Microporous Mesoporous Mater. 109 (2008) 305–316, https://doi.org/10.1016/j.micromeso.2007.05.005.

[39] S. Brunauer, P.H. Emmet, E. Teller, Adsorption of gases in multimolecular layers, J. Am. Soc. 60 (1938) 309–319, https://doi.org/10.1021/ja01269a023.

[40] J. Jagiello, J.P. Olivier, 2D-NLDFT adsorption models for carbon slit-shaped pores with surface energetical heterogeneity and geometrical corrugation, Carbon 55 (2013) 70–80, https://doi.org/10.1016/j.carbon.2012.12.011.

[41] I. Such-Basáñez, M.C. Román-Martínez, C. Salinas-Martínez de Lecea, Ligand adsorption on different activated carbon materials for catalyst anchorage, Carbon 42 (7) (2004) 1357–1361.

[42] M. Thommes, K. Kaneko, A.V. Neimark, J.P. Olivier, F. Rodriguez-Reinoso, J. Rouquerol, K.S.W. Sing, Physisorption of gases, with special reference to the evaluation of surface area and pore size distribution (IUPAC Technical Report), Pure Appl. Chem. 87 (2015) 1051–1069, https://doi.org/10.1515/pac-2014-1117.

[43] M. Gineys, R. Benoit, N. Cohaut, F. Béguin, S. Delpeux-Ouldriane, Behavior of activated carbon cloths used as electrode in electrochemical processes, Chem. Eng. J. 310 (2017) 1–12, https://doi.org/10.1016/j.cej.2016.10.018.

[44] X. Ye, W. Cai, D. Lu, R. Liu, Y. Wu, Y. Wang, Electrochemical regeneration of granular activated carbon using an AQS (9,10-anthraquinone-2-sulfonic acid)/PPy modified graphite plate cathode, Chemosphere 308 (2022), 136189, https://doi.org/10.1016/j.chemosphere.2022.136189.

[45] A. Khataee, S. Sajjadi, S.R. Pouran, A. Hasanzadeh, S.W. Joo, A comparative study on electrogeneration of hydrogen peroxide through oxygen reduction over various plasma-treated graphite electrodes, Electrochim. Acta 244 (2017) 38–46, https://doi.org/10.1016/j.electacta.2017.05.069.

[46] B. Karabacakoğlu, Ö. Savlak, Electrochemical Regeneration of Cr(VI) Saturated granular and powder activated carbon: comparison of regeneration efficiency, Ind. Eng. Chem. Res. 53 (2014) 13171–13179, https://doi.org/10.1021/ie500161d.

[47] C.A. Martínez-Huitle, M.A. Rodrigo, I. Sirés, O. Scialdone, Single and coupled electrochemical processes and reactors for the abatement of organic water pollutants: A Critical Review, Chem. Rev. 115 (2015) 13362–13407, https://doi.org/10.1021/acs.chemrev.5b00361.

[48] H. Monteil, Y. Pechaud, N. Oturan, C. Trellu, M.A. Oturan, Pilot scale continuous reactor for water treatment by electrochemical advanced oxidation processes: Development of a new hydrodynamic/reactive combined model, Chem. Eng. J. 404 (2021), 127048, https://doi.org/10.1016/j.cej.2020.127048.

[49] A. Larasati, G.D. Fowler, N.J.D. Graham, Insights into chemical regeneration of activated carbon for water treatment, J. Environ. Chem. Eng. 9 (4) (2021) 105555.

[50] P.-Z. Cheng, H. Teng, Electrochemical responses from surface oxides present on HNO₃-treated carbons, Carbon 41 (2003) 2057–2063, https://doi.org/10.1016/S0008-6223(03)00212-4.

[51] M.J. Bleda-Martínez, D. Lozano-Castelló, E. Morallón, D. Cazorla-Amorós, A. Linares-Solano, Chemical and electrochemical characterization of porous carbon materials, Carbon 44 (2006) 2642–2651, https://doi.org/10.1016/j.carbon.2006.04.017.

[52] A.C. Lazanas, M.I. Prodromidis, Electrochemical impedance spectroscopy – a tutorial, ACS Meas. Sci. Au. 3 (2023) 162–193, https://doi.org/10.1021/acsmeasuresciau.2c00070.

[53] R. Kötz, M. Carlen, Principles and applications of electrochemical capacitors, Electrochim. Acta 45 (2000) 2483–2498, https://doi.org/10.1016/S0013-4686(00)00354-6.

[54] B.E. Conway, Electrochemical supercapacitors: Scientific Fundamentals and Technological Applications. New York: Springer; 1999. https://doi.org/10.1007/978-1-4757-3058-6.